Zygote **25** (October), pp. 575–582. © Cambridge University Press 2017
doi:10.1017/S0967199417000405 First Published Online 11 July 2017

Acetylation and methylation profiles of H3K27 in porcine embryos cultured *in vitro*

Luciana Simões Rafagnin Marinho[2], *Vitor Braga Rissi*[3], *Andressa Guidugli Lindquist*[2], *Marcelo Marcondes Seneda*[1] *and Vilceu Bordignon*[4]

Laboratory of Animal Reproduction, UEL, Rodovia Celso Garcia Cid, Campus Universitário, Londrina, Brazil; Laboratory of Biotechnology and Animal Reproduction – BioRep, Veterinary Hospital, Federal University of Santa Maria, Santa Maria, Brazil; and Department of Animal Science, McGill University, Sainte Anne de Bellevue, Quebec, Canada

Date submitted: 22.03.2017. Date revised: 20.05.2017. Date accepted: 25.05.2017

Summary

Methylation and acetylation of histone H3 at lysine 27 (H3K27) regulate chromatin structure and gene expression during early embryo development. While H3K27 acetylation (H3K27ac) is associated with active gene expression, H3K27 methylation (H3K27me) is linked to transcriptional repression. The aim of this study was to assess the profile of H3K27 acetylation and methylation (mono-, di- and trimethyl) during oocyte maturation and early development *in vitro* of porcine embryos. Oocytes/embryos were fixed at different developmental stages from germinal vesicle to day 8 blastocysts and submitted to an immunocytochemistry protocol to identify the presence and quantify the immunofluorescence intensity of H3K27ac, H3K27me1, H3K27me2 and H3K27me3. A strong fluorescent signal for H3K27ac was observed in all developmental stages. H3K27me1 and H3K27me2 were detected in oocytes, but the fluorescent signal decreased through the cleavage stages and rose again at the blastocyst stage. H3K27me3 was detected in oocytes, in only one pronucleus in zygotes, cleaved-stage embryos and blastocysts. The nuclear fluorescence signal for H3K27me3 increased from the 2-cell stage to 4-cell stage embryos, decreased at the 8-cell and morula stages and increased again in blastocysts. Different patterns of the H3K27me3 mark were observed at the blastocyst stage. Our results suggest that changes in the H3K27 methylation status regulate early porcine embryo development as previously shown in other species.

Keywords: Embryo development, Gene expression, H3K27 acetylation, H3K27 methylation, Swine

Introduction

Normal embryo development involves important rearrangements in the chromatin structure. This change includes a global reprogramming of epigenetic marks starting following fertilization, which is required to create a totipotent state zygote (Fraser & Lin, 2016). Epigenetic marks are essential elements of the cell machinery that functionally interprets DNA sequences. These marks contribute to the establishment of cell identity by regulating gene expression patterns that are specific for each cell lineage (Chen & Pei, 2016). In addition to regulate gene expression, epigenetic marks are also involved in the regulation of other critical events during embryogenesis in mammals, including genomic imprinting, inactivation of the X chromosome and reprogramming of the two parental haploid genomes into one diploid genome (Morris, 2009; Hales *et al.*, 2011).

Important epigenetic marks involved in the regulation of early embryo development include DNA methylation, non-coding RNAs and post-translational modifications of specific residues in nucleosomal

[1]All correspondence to: Marcelo Marcondes Seneda. Laboratory of Animal Reproduction, State University of Londrina (UEL), Rodovia Celso Garcia Cid, Km 380, s/n – Campus Universitário, CEP 86057–970, Londrina, PR, Brazil. E-mail: marcelo.seneda@gmail.com
[2]Laboratory of Animal Reproduction, State University of Londrina (UEL), Rodovia Celso Garcia Cid, Km 380, s/n – Campus Universitário, CEP 86057–970, Londrina, PR, Brazil
[3]Laboratory of Biotechnology and Animal Reproduction – BioRep, Veterinary Hospital, Federal University of Santa Maria, Av. Roraima, 1000 – Camobi, CEP 97105–900, Santa Maria, RS, Brazil
[4]Department of Animal Science, McGill University, 21111 Lakeshore Road, Sainte Anne de Bellevue, Quebec H9X 3V9, Canada

histones, such as acetylation and methylation (Novina & Sharp, 2004; Cook & Blelloch, 2013; Beaujean, 2014; Dallaire & Simard, 2016; Ambrosi *et al.*, 2017). Histone acetylation usually occurs on the lysine residues of core histones and neutralizes the basic charge of these residues, therefore decreasing their affinity for DNA (Hasan & Hottiger, 2002). Histone acetylation is almost invariably associated with activation of gene transcription, and is involved in the regulation of cell totipotency and proliferation events during cell reprogramming and embryo development (Wang *et al.*, 2007; Rodriguez-Sanz *et al.*, 2014). For instance, acetylation of histone H3 at lysine 27 (H3K27ac) plays an important role in the maintenance of pluripotency and regulation of key developmental genes in stem cells (Creyghton *et al.*, 2010; Pasini *et al.*, 2010).

Conversely, methylation of H3K27 (H3K27me) is usually associated with transcriptional repression, promoting stable and heritable gene silencing (Schwartz & Pirrotta, 2007). Trimethylation of H3K27 (H3K27me3) regulates lineage specification by temporarily repressing genes involved in development and cell differentiation of pluripotent cells (Surface *et al.*, 2010; Shpargel *et al.*, 2014). Indeed, genes associated to organogenesis, morphogenesis and embryonic development are temporarily suppressed by H3K27me3 until the time when their transcription is required (Boyer *et al.*, 2006).

It is well established that mammalian embryos undergo several epigenetic modifications during early development (Boland *et al.*, 2014). Nonetheless, the regulatory mechanism of lineage commitment is still not fully known. Understanding how different species organize their chromatin following fertilization is fundamental for comprehending the epigenetic regulation of early embryonic development and may help to determine improved conditions for *in vitro* embryo production. Therefore, the objective of this study was to evaluate the profile of acetylation and methylation of histone H3 at lysine 27 during oocyte maturation and early development *in vitro* of porcine embryos.

Materials and Methods

Unless otherwise indicated, chemicals were purchased from Sigma Chemical Company (Sigma-Aldrich, Oakville, ON, Canada).

Oocyte collection and *in vitro* maturation

Ovaries from prepubertal gilts were collected from a local abattoir and transported to the laboratory in 0.9% NaCl at 30 to 35°C. Cumulus–oocyte complexes (COCs) were aspirated from 3-mm to 6-mm diameter follicles using an 18-gauge needle. Only COCs surrounded by a minimum of three cumulus-cell layers, with an evenly granulated cytoplasm were selected for *in vitro* maturation (IVM). Groups of 20 to 25 COCs were cultured in 100 µl of maturation medium under mineral oil, in a humidified atmosphere of 5% CO_2 and 95% air at 38.5°C. Maturation medium consisted of TCM-199 (Life Technologies, Burlington, ON, Canada), supplemented with 0.1 mg/ml cysteine, 0.91 mM sodium pyruvate, 3.05 mM D-glucose, 0.5 µg/ml follicle-stimulating hormone (FSH; SIOUX Biochemical Inc.), 0.5 µg/ml luteinizing hormone (LH, SIOUX Biochemical Inc.), 10 ng/ml epidermal growth factor (EGF; Life Technologies), 20 µg/ml gentamicin (Life Technologies), 1 mM dibutyryl cyclic adenosine monophosphate (dbcAMP), and 20% (v/v) porcine follicular fluid. After 22 h, the oocytes were transferred to the same maturation medium, but without FSH, LH, and dbcAMP for an additional 22 to 24 h, under the same conditions.

In vitro fertilization (IVF) and *in vitro* culture (IVC)

Matured oocytes were freed from cumulus cells by vortexing in TCM 199 HEPES-buffered medium (Life Technologies) supplemented with 0.1% hyaluronidase for 7 min. The denuded oocytes were washed in the same medium before being transferred to fertilization medium.

The oocytes were washed twice in fertilization medium, which consisted of Tris-buffered medium (TBM) supplemented with 2.5 mg/ml fatty acid-free bovine serum albumin (BSA), and placed in 90 µl drops of the same medium. A pool of fresh semen collected from 3–4 fertile boars was left at 18°C for 24 h and then centrifuged at 4000 rpm for 3 min. Supernatant was discarded and the sperm pellet was re-suspended in 1 ml of fertilization medium and homogenized. The semen was centrifuged again (4000 rpm for 2 min), the supernatant was discarded and the sperm pellet was re-suspended in 500 µl of fertilization medium. Sperm concentration was adjusted to obtain a final concentration of 2,000 live sperm/oocyte. Sperm and oocytes were co-incubated for 4 h under mineral oil at 38.5°C, in 5% CO_2 in air and 100% humidity.

After IVF, the oocytes were washed three times in porcine zygote medium (PZM-3) supplemented with 3 mg/ml BSA and then cultured in the same medium under mineral oil. Culture conditions were humidified atmosphere of 5% CO_2 and 95% air at 38.5°C. Cleavage and blastocyst rates were determined at 48 h and 7 days after IVF, respectively.

Immunocytochemistry

Oocytes/embryos were fixed at the following developmental stages: germinal vesicle (GV) and metaphase II

https://doi.org/10.1017/S0967199417000405 Published online by Cambridge University Press

(MII) oocytes, pronuclear (PN; 18 hours post fertilization – hpf), 2-cell stage (2C; 36 hpf), 4-cell stage (4C; 48 hpf), 8-cell stage (8C; 72 hpf), D6 blastocysts (D6; 144 hpf) and D8 blastocysts (D8; 192 hpf). Samples were rinsed in PBS, fixed in 4% paraformaldehyde for 15 to 20 min and stored at 4°C in PBS with 0.2% TritonX-100 and 0.3% BSA. Cell permeabilization was performed with 0.5% Triton X-100 in PBS with 0.3% BSA for 1 h at 37°C. Oocytes/embryos were then washed twice (10 min each) in blocking solution (3% BSA and 0.2% Tween-20 in PBS) and exposed overnight at 4°C to primary antibodies diluted in blocking solution (1:1000). Polyclonal rabbit anti-H3K27 acetyl (Abcam; ab4729), anti-monomethyl H3K27 (Upstate; 07–448), anti-dimethyl H3K27 (Upstate; 07–452), and anti-trimethyl H3K27 (Upstate; 07–449) were used as primary antibodies. Samples were then washed three times for 20 min each in blocking solution and incubated for 2 h at room temperature in the presence of 1:1000 diluted Alexa Flour 488 goat anti-rabbit (Molecular Probes, Eugene, OR, USA) secondary antibodies. Finally, the samples were washed three times (20 min each) in blocking solution. For the second wash, the solution was supplemented with 10 µg/ml DAPI (4′,6-diamidino-2-phenylindole) for DNA staining. Oocytes/embryos were mounted on microscope slides using a drop of Mowiol and examined by epifluorescence using a Nikon eclipse 80i microscope (Nikon, Tokyo, Japan) with ×200 magnification. Images were individually recorded using a Retiga 2000R monochrome digital camera (Qimaging, BC, Canada). The exposure gains and rates were consistent between samples. Fluorescence intensities were quantified by using Image J analysis (Schneider *et al.*, 2012). Control samples from each developmental stage were processed as described above, but the primary antibody was omitted. Images from 183 oocytes/embryos were analyzed.

Results

H3K27ac was detected in the nuclei of GV and in the DNA of MII oocytes. Strong fluorescent signals were observed in both PN and in 2C and 4C stages. The fluorescent signal decreased at the 8C stage but increased again in D6 and D8 blastocysts (Figs 1 and 2).

The fluorescent signal for H3K27me1 was intense in GV and MII oocytes, but decreased markedly in cleaved-stage embryos. The fluorescent signal was barely detectable in zygotes, 2C, 4C and 8C embryos, but intensity increased in D6 and D8 blastocysts (Figs 1 and 2).

H3K27me2 revealed a strong fluorescent signal in GV and MII stage oocytes, but very weak or absent signal in PN of zygotes. Cleaved-stage embryos showed weak or no fluorescent signal for H3K27me2, but all nuclei were H3K27me2 positive in D6 and D8 blastocysts (Figs 1 and 2).

Strong fluorescence intensity for H3K27me3 was detected in GV and MII oocytes. In zygotes, only one of the pronuclei was H3K27me3 positive (Fig. 3). H3K27me3 signal was detected in 2C and 4C stages, but 8C embryos and D6 blastocysts showed very weak or no fluorescent signal (Figs 1 and 2). The fluorescent pattern in D8 blastocyst varied from absence of fluorescent signal (7 embryos), mixture of fluorescent positive and negative cells (19 embryos), to only inner cell mass (ICM) positive staining (three embryos; Fig. 4).

Discussion

Epigenetic changes are known to regulate the programming of the genetic information carried over by the oocyte and the sperm to the new developing embryo and control totipotency and cell lineage commitment (Lu & Zhang, 2015; Ancelin *et al.*, 2016). To gain additional insights into the epigenetics changes that occur at early embryo stages we have evaluated the global profile of H3K27 acetylation, mono-, di-, and trimethylation during *in vitro* development of porcine embryos. H3K27 methylation is catalyzed by the transcriptional repressors Polycomb group (PcG) proteins, which form two chromatin modifying complexes, Polycomb Repressive Complex 1 and Complex 2 (PRC1 and PRC2) (O'Meara & Simon, 2012; Williams *et al.*, 2014). Removal of this epigenetic mark can make undifferentiated normal (Patel *et al.*, 2012) or cancerous cells (Gannon *et al.*, 2013; Ciarapica *et al.*, 2014) susceptible to differentiation. H3K27me3 is a Polycomb repressed state, which is functionally opposed by actively transcribed chromatin (O'Meara & Simon, 2012). Conversely, H3K27ac is generally enriched in promoters of active genes (Tie *et al.*, 2009; O'Meara & Simon, 2012) and can antagonize PcG activity by competing with the placement of the H3K27me3 mark (Schwartz *et al.*, 2010). Consistent with this, it has been shown that H3K27ac and H3K27me3 have dynamic and complementary temporal profiles during embryogenesis (Tie *et al.*, 2009).

In this study, H3K27me3 was detected in immature and matured oocytes, which is in accordance with others studies in pigs (Park *et al.*, 2009; Cao *et al.*, 2015; Xie *et al.*, 2016) and cattle (Ross *et al.*, 2008). In zygotes, only one of the two pronuclei was positive for this mark. A similar pattern of H3K27me3 staining in zygotes was reported in other studies in pigs (Young *et al.*, 2007; Park *et al.*, 2009), cattle (Breton *et al.*, 2010) and mice (Erhardt *et al.*, 2003; Santos *et al.*, 2005). We believe that the H3K27me3 positive was the female

https://doi.org/10.1017/S0967199417000405 Published online by Cambridge University Press

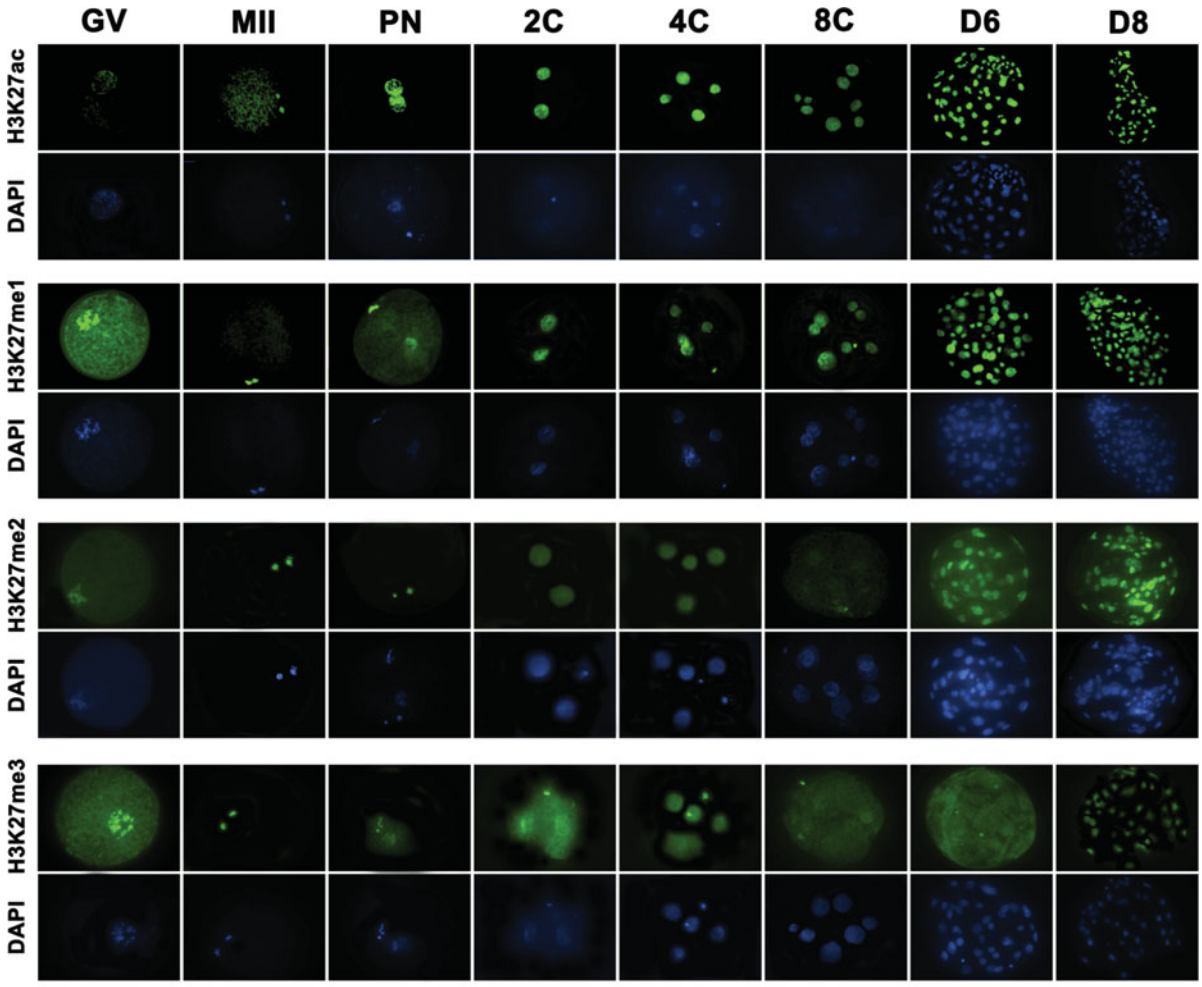

Figure 1 Distribution of acetylated, mono-, di- and tri-methylated H3K27 in porcine oocytes and embryos. Panels show representative images of immature (GV stage) and mature (MII stage) oocytes, zygotes (PN stage), 2-cell (2C), 4-cell (4C) and 8-cell (8C) stage embryos, and day 6 (D6) and day 8 (D8) blastocysts.

PN given that polyspermic zygotes having more than two PNs also contained only one positive PN. However, Ross *et al.* (2008) observed an asymmetric staining pattern in bovine embryos at PN stage and proposed that the female PN was the one positive for H3K27me3. They have also observed that both pronuclei in parthenogenetically activated embryos were H3K27me3 positive, which further confirms that the positive PN in fertilized zygotes is derived from the oocyte.

We have observed that the fluorescent intensity for H3K27me3 decreases at the 8-cell stage. This finding is in line with other reports in porcine (Park *et al.*, 2009) and bovine embryos (Ross *et al.*, 2008; Breton *et al.*, 2010). Interestingly, we observed different patterns of H3K27me3 fluorescent staining in D8 blastocysts, which included embryos with no stained cells, embryos with a mix of positive and negative cells, embryos with all the cells stained, and embryos with only the ICM stained. A previous study by Park *et al.* (2009) did not detect H3K27me3 in porcine blastocysts at D6 of development (144 hpf). Conversely, Gao *et al.*, (2010) reported that levels of H3K27me3 increased in hatched blastocysts. Along with our observations, data from those studies suggest that H3K27me3 pattern in porcine blastocysts may differ from other species given that intense fluorescence signal for H3K27me3 was found in bovine (Ross *et al.*, 2008) and murine (Erhardt *et al.*, 2003) blastocysts.

Monomethylated H3K27 was detectable in GV and MII stage oocytes, which is in agreement with a previous study in porcine embryos (Park *et al.*, 2009). However, we observed that H3K27me1 was present in only one PN, while similar fluorescent signal in both PNs was reported in the previous study (Park *et al.*, 2009). As H3K27me1 becomes detectable in the male pronucleus several hours after fertilization, one possibility is that the pronuclear development stage of zygotes evaluated in our study was different from the previous study. In mice, H3K27me1 signal

https://doi.org/10.1017/S0967199417000405 Published online by Cambridge University Press

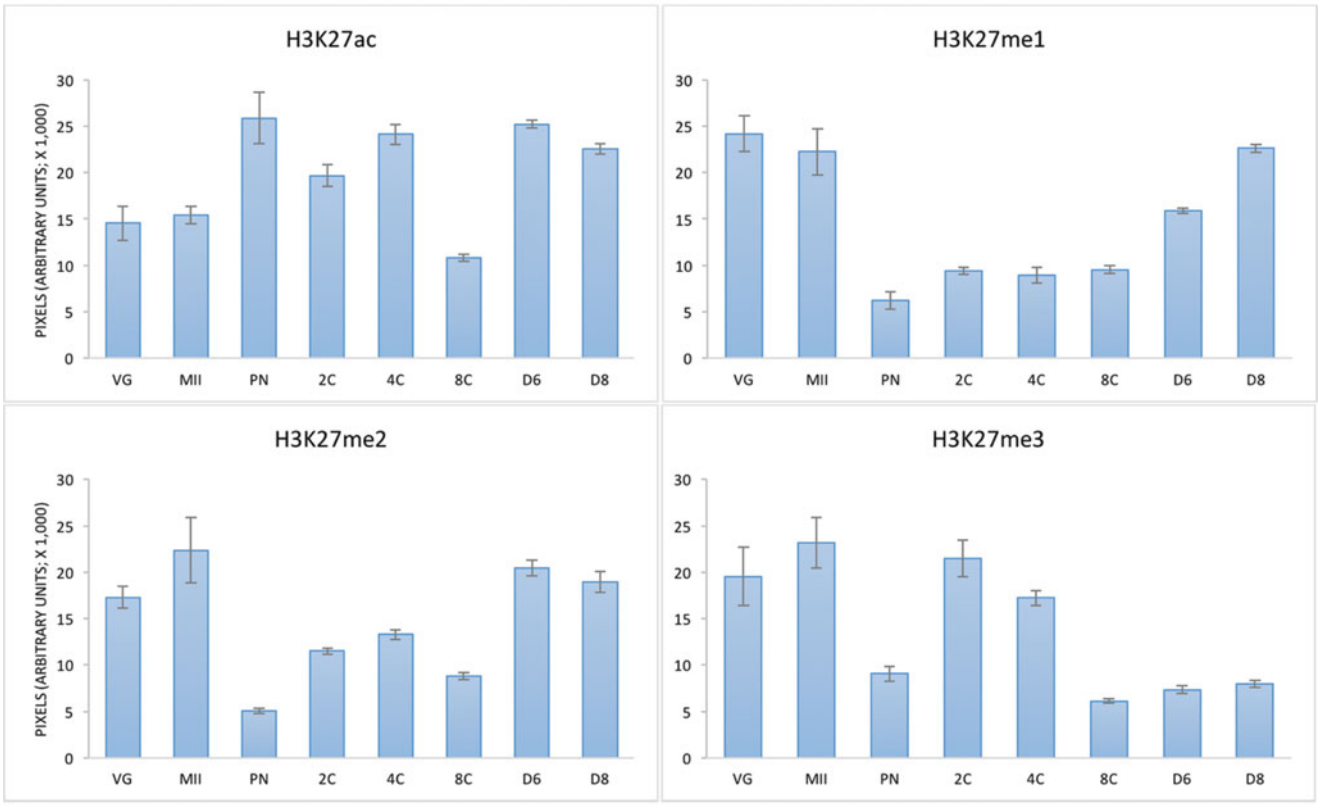

Figure 2 Fluorescence intensity for H3K27ac (A), H3K27me1 (B), H3K27me2 (C) and H3K27me3 (D) in porcine oocytes and developing embryos. GV = germinal vesicle oocytes, MII = metaphase II oocytes, PN = pronuclear stage zygotes, 2C = two-cell stage embryos, 4C = four-cell stage embryos, 8C = eight-cell stage embryos, D6 = day 6 blastocysts, D8 = day 8 blastocysts.

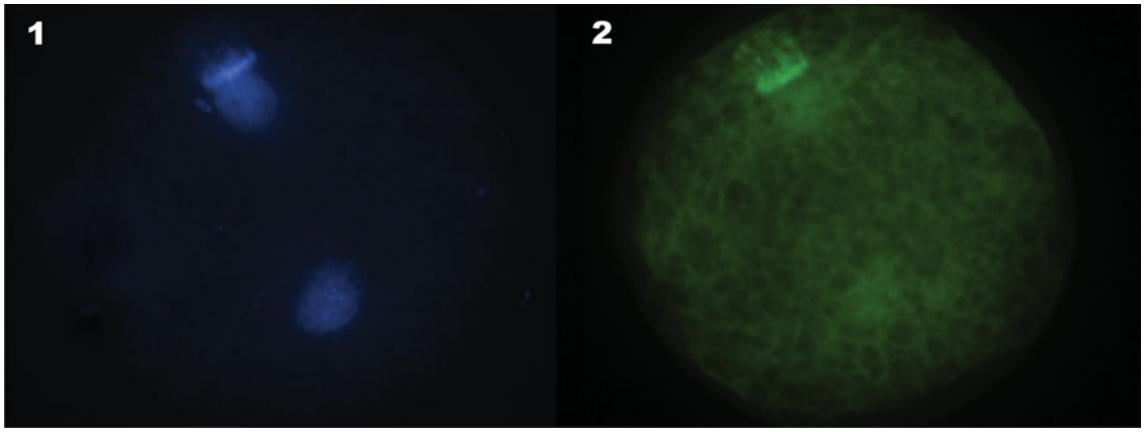

Figure 3 H3K27me3 immunofluorescence image of a polyspermic zygote showing one stained and two non-stained PNs. (1) DNA stained with DAPI. (2) H3K27me3 fluorescent signal.

is mainly present in the female PN (Erhardt *et al.*, 2003; Van Der Heijden *et al.*, 2005), but the signal increased during male PN formation (Erhardt *et al.*, 2003; Santos *et al.*, 2005; Van Der Heijden *et al.*, 2005). The H3K27me1signal from 2C to the blastocyst stage observed in this study corroborates with findings from a previous study (Park *et al.*, 2009).

We observed absence or weak fluorescent intensity for H3K27me2 in zygotes, which differs from previous studies in mice reporting intensive H3K27me2 signal in PNs of mice zygotes (Erhardt *et al.*, 2003). Conversely, we observed a prominent fluorescent signal for H3K27me2 in D6 and D8 IVF blastocysts, while another study reported that H3K27me2 levels were

https://doi.org/10.1017/S0967199417000405 Published online by Cambridge University Press

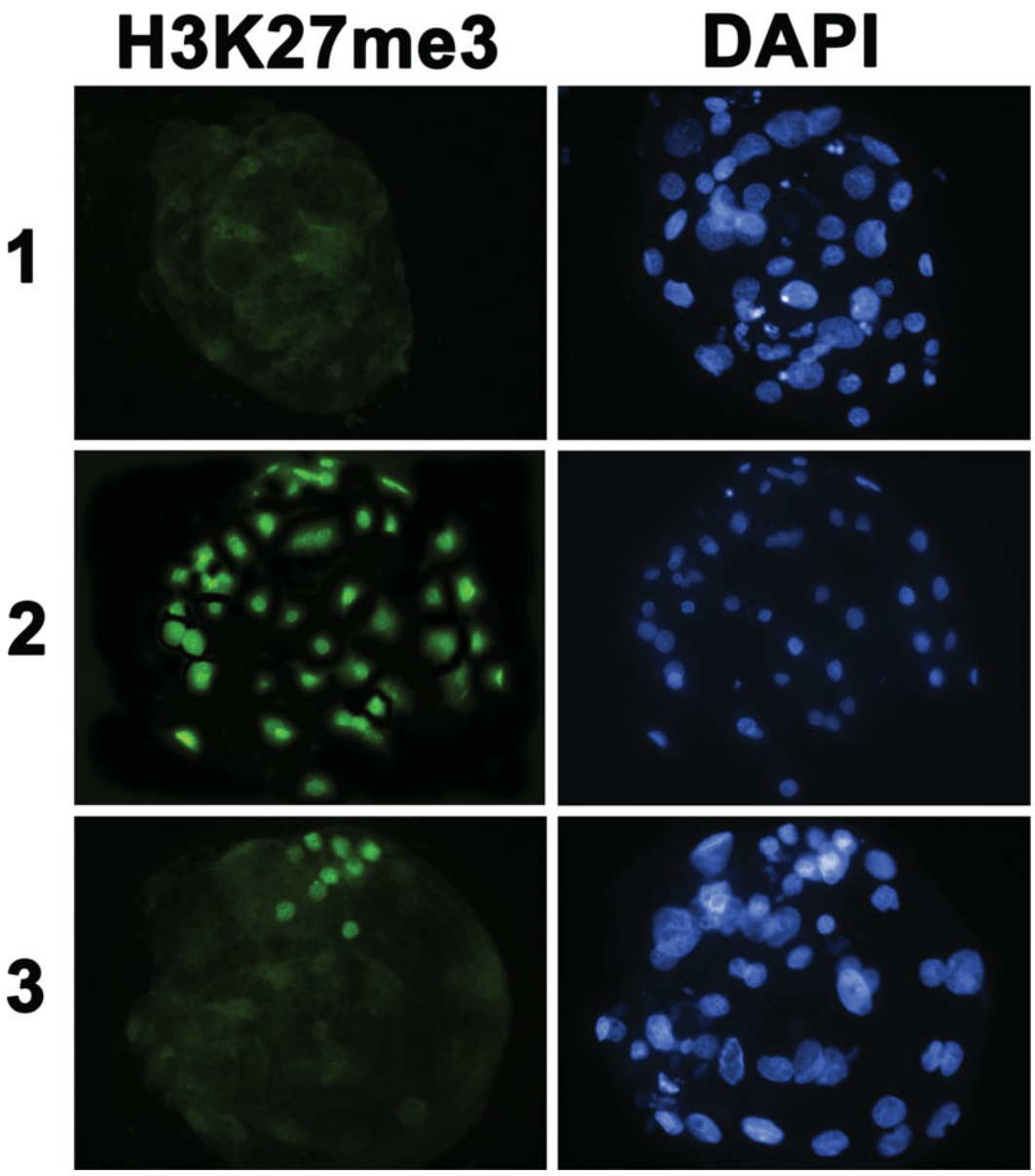

Figure 4 H3K27me3 immunofluorescence image day 8 blastocysts. (1) Embryo with absence or weak H3K27me3 fluorescent signal. (2) Embryo with strong H3K27me3 fluorescent signal in all the cells. (3) Embryo with strong H3K27me3 fluorescent signal only in the ICM cells.

nearly undetectable in porcine blastocysts produced by parthenogenetic activation (Huang *et al.*, 2015). Differences between fertilized and parthenogenetic embryos have been reported regarding other histone modifications including H3K9ac and H3K27ac (Huang *et al.*, 2015).

Intensive fluorescent signal for H3K27ac was observed in oocytes, in both PNs of zygotes, and all developmental stages from 2C to blastocyst. However, the intensity of the fluorescent signal decreased in 8C-stage embryos. A similar pattern of H3K27ac in porcine embryos was reported in a previous study by Zhou *et al.* (2014).

In summary, our study revealed that the global pattern of acetylation and mono-, di- and trimethylation of the H3K27 changes during *in vitro* development of porcine embryos. Based on published literature, our findings suggest that porcine embryos produced by IVF may differ from embryos of other species regarding the global changes in H3K27, including the pattern of H3K27me3 at the blastocyst stage and H3K27me2 in zygotes. Our findings may provide a base for further investigation of the mechanistic relevance of each epigenetic change occurring in the H3K27 for the regulation of early embryo development.

https://doi.org/10.1017/S0967199417000405 Published online by Cambridge University Press

References

Ambrosi, C., Manzo, M. & Baubec, T. (2017). Dynamics and context-dependent roles of DNA methylation. *J. Mol. Biol.* **429**, 1459–75.

Ancelin, K., Syx, L., Borensztein, M., Ranisavljevic, N., Vassilev, I., Briseno-Roa, L., Liu, T., Metzger, E., Servant, N., Barillot, E., *et al*. (2016). Maternal LSD1/KDM1A is an essential regulator of chromatin and transcription landscapes during zygotic genome activation. *Elife* **5**, pii: e08851.

Beaujean, N. (2014). Histone post-translational modifications in preimplantation mouse embryos and their role in nuclear architecture. *Mol. Reprod. Dev.* **81**, 100–12.

Boland, M.J., Nazor, K.L. & Loring, J.F. (2014). Epigenetic regulation of pluripotency and differentiation. *Circ. Res.* **115**, 311–324.

Boyer, L.A., Plath, K., Zeitlinger, J., Brambrink, T., Medeiros, L.A., Lee, T.I., Levine, S.S., Wernig, M., Tajonar, A., Ray, M.K., *et al*. (2006). Polycomb complexes repress developmental regulators in murine embryonic stem cells. *Nature* **441**, 349–53.

Breton, A., LE Bourhis, D., Audouard, C., Vignon, X. & Lelièvre, J.-M. (2010). Nuclear profiles of H3 histones trimethylated on Lys27 in bovine (*Bos taurus*) embryos obtained after *in vitro* fertilization or somatic cell nuclear transfer. *J. Reprod. Dev*. **56**, 379–88.

Cao, Z., Li, Y., Chen, Z., Wang, H., Zhang, M., Zhou, N., Wu, R., Ling, Y., Fang, F., Li, N., *et al*. (2015). Genome-wide dynamic profiling of histone methylation during nuclear transfer-mediated porcine somatic cell reprogramming. *PLoS One* **10**, e0144897.

Chen, J. & Pei, D. (2016). Epigenetic landmarks during somatic reprogramming. *IUBMB Life* **68**, 854–7.

Ciarapica, R., Carcarino, E., Adesso, L., De Salvo, M., Bracaglia, G., Leoncini, P.P., Dall'agnese, A., Verginelli, F., Milano, G.M., Boldrini, R., *et al*. (2014). Pharmacological inhibition of EZH2 as a promising differentiation therapy in embryonal RMS. *BMC Cancer* **14**, 139.

Cook, M.S. & Blelloch, R. (2013). Small RNAs in germline development. *Curr. Top. Dev. Biol.* **102**, 159–205.

Creyghton, M.P., Cheng, A.W., Welstead, G.G., Kooistra, T., Carey, B.W., Steine, E.J., Hanna, J., Lodato, M. a, Frampton, G.M., Sharp, P.A., *et al*. (2010). Histone H3K27ac separates active from poised enhancers and predicts developmental state. *Proc. Natl. Acad. Sci. USA* **107**, 21931–6.

Dallaire, A. & Simard, M.J. (2016). The implication of microRNAs and endo-siRNAs in animal germline and early development. *Dev. Biol.* **416**, 18–25.

Erhardt, S., Su, I.-H., Schneider, R., Barton, S., Bannister, A.J., Perez-Burgos, L., Jenuwein, T., Kouzarides, T., Tarakhovsky, A. & Surani, M.A. (2003). Consequences of the depletion of zygotic and embryonic enhancer of zeste 2 during preimplantation mouse development. *Development* **130**, 4235–48.

Fraser, R. & Lin, C.-J. (2016). Epigenetic reprogramming of the zygote in mice and men: on your marks, get set, go! *Reproduction* **152**, R211–22.

Gannon, O.M., De Long, L.M., Endo-Munoz, L., Hazar-Rethinam, M. & Saunders, N.A. (2013). Dysregulation of the repressive H3K27 trimethylation mark in head and neck squamous cell carcinoma contributes to dysregulated squamous differentiation. *Clin. Cancer Res.* **19**, 428–41.

Gao, Y., Hyttel, P. & Hall, V.J. (2010). Regulation of H3K27me3 and H3K4me3 during early porcine embryonic development. *Mol. Reprod. Dev.* **77**, 540–9.

Hales, B.F., Grenier, L., Lalancette, C. & Robaire, B. (2011). Epigenetic programming: From gametes to blastocyst. *Birth Defects Res. Part A - Clin. Mol. Teratol.* **91**, 652–65.

Hasan, S. & Hottiger, M.O. (2002). Histone acetyl transferases: a role in DNA repair and DNA replication. *J. Mol. Med.* **80**, 463–74.

Huang, Y., Yuan, L., Li, T., Wang, A., Li, Z., Pang, D., Wang, B. & Ouyang, H. (2015). Valproic acid improves porcine parthenogenetic embryo development through transient remodeling of histone modifiers. *Cell. Physiol. Biochem.* **37**, 1463–73.

Lu, F. & Zhang, Y. (2015). Cell totipotency: molecular features, induction, and maintenance. *Natl. Sci. Rev.* **2**, 217–25.

Morris, K. (2009). Non-coding RNAs, epigenetic memory and the passage of information to progeny. *RNA Biol*. **6**, 242–7.

Novina, C.D. & Sharp, P.A. (2004). The RNAi revolution. *Nature* **430**, 161–4.

O'Meara, M.M. & Simon, J.A. (2012). Inner workings and regulatory inputs that control Polycomb repressive complex 2. *Chromosoma* **121**, 221–34.

Park, K.E., Magnani, L. & Cabot, R.A. (2009). Differential remodeling of mono- and trimethylated H3K27 during porcine embryo development. *Mol. Reprod. Dev.* **76**, 1033–42.

Pasini, D., Malatesta, M., Jung, H.R., Walfridsson, J., Willer, A., Olsson, L., Skotte, J., Wutz, A., Porse, B., Jensen, O.N., *et al*. (2010). Characterization of an antagonistic switch between histone H3 lysine 27 methylation and acetylation in the transcriptional regulation of Polycomb group target genes. *Nucleic Acids Res*. **38**, 4958–69.

Patel, T., Tursun, B., Rahe, D.P. & Hobert, O. (2012). Removal of Polycomb repressive complex 2 makes C. elegans germ cells susceptible to direct conversion into specific somatic cell types. *Cell Rep*. **2**, 1178–86.

Rodriguez-Sanz, H., Moreno-Romero, J., Solis, M.-T., Kohler, C., Risueno, M.C. & Testillano, P.S. (2014). Changes in histone methylation and acetylation during microspore reprogramming to embryogenesis occur concomitantly with Bn HKMT and Bn HAT expression and are associated with cell totipotency, proliferation & differentiation in *Brassica napus*. *Cytogenet. Genome Res.* **143**, 209–18.

Ross, P.J., Ragina, N.P., Rodriguez, R.M., Iager, A.E., Siripattarapravat, K., Lopez-Corrales, N. & Cibelli, J.B. (2008). Polycomb gene expression and histone H3 lysine 27 trimethylation changes during bovine preimplantation development. *Reproduction* **136**, 777–85.

Santos, F., Peters, A.H., Otte, A.P., Reik, W. & Dean, W. (2005). Dynamic chromatin modifications characterise the first cell cycle in mouse embryos. *Dev. Biol.* **280**, 225–236.

Schneider, C.A., Rasband, W.S. & Eliceiri, K.W. (2012). NIH Image to ImageJ: 25 years of image analysis. *Nat. Methods* **9**, 671–5.

Schwartz, Y.B. & Pirrotta, V. (2007). Polycomb silencing mechanisms and the management of genomic programmes. *Nat. Rev. Genet.* **8**, 9–22.

Schwartz, Y.B., Kahn, T.G., Stenberg, P., Ohno, K., Bourgon, R. & Pirrotta, V. (2010). Alternative epigenetic chromatin states of Polycomb target genes. *PLoS Genet*. **6**, e1000805.

Shpargel, K.B., Starmer, J., Yee, D., Pohlers, M. & Magnuson, T. (2014). KDM6 demethylase independent loss of histone H3 lysine 27 trimethylation during early embryonic development. *PLoS Genet*. **10**, e1004507.

Surface, L.E., Thornton, S.R. & Boyer, L.A. (2010). Polycomb group proteins set the stage for early lineage commitment. *Cell Stem Cell* **7**, 288–98.

Tie, F., Banerjee, R., Stratton, C. a, Prasad-Sinha, J., Stepanik, V., Zlobin, A., Diaz, M.O., Scacheri, P.C. & Harte, P.J. (2009). CBP-mediated acetylation of histone H3 lysine 27 antagonizes *Drosophila* Polycomb silencing. *Development* **136**, 3131–41.

Van Der Heijden, G.W., Dieker, J.W., Derijck, A.A.H.A., Muller, S., Berden, J.H.M., Braat, D.D.M., Van Der Vlag, J. & De Boer, P. (2005). Asymmetry in Histone H3 variants and lysine methylation between paternal and maternal chromatin of the early mouse zygote. *Mech. Dev*. **122**, 1008–22.

Wang, F., Kou, Z., Zhang, Y. & Gao, S. (2007). Dynamic reprogramming of histone acetylation and methylation in the first cell cycle of cloned mouse embryos. *Biol. Reprod.* **77**, 1007–16.

Williams, K., Christensen, J., Rappsilber, J., Nielsen, A.L., Johansen, J.V. & Helin, K. (2014). The histone lysine demethylase JMJD3/KDM6B is recruited to p53 bound promoters and enhancer elements in a p53 dependent manner. *PLoS One* **9**, e96545.

Xie, B., Zhang, H., Wei, R., Li, Q., Weng, X., Kong, Q. & Liu, Z. (2016). Histone H3 lysine 27 trimethylation acts as an epigenetic barrier in porcine nuclear reprogramming. *Reproduction* **151**, 9–16.

Young, S.J., Yeo, S., Jung, S.P., Lee, K.K. & Kang, Y.K. (2007). Gradual development of a genome-wide H3-K9 trimethylation pattern in paternally derived pig pronucleus. *Dev. Dyn.* **236**, 1509–16.

Zhou, N., Cao, Z., Wu, R., Liu, X., Tao, J., Chen, Z., Song, D., Han, F., Li, Y., Fang, F., *et al*. (2014). Dynamic changes of histone H3 lysine 27 acetylation in pre-implantational pig embryos derived from somatic cell nuclear transfer. *Anim. Reprod. Sci.* **148**, 153–63.